ADDENDUM

Exploring the Energy Frontier with Deep Inelastic Scattering at the LHC

A Contribution to the Update of the European Strategy on Particle Physics

Sent in confidence to the Strategy Secretariat

LHeC and PERLE Collaboration

Contacts: Oliver Brüning (CERN) and Max Klein (U Liverpool)
oliver.bruning@cern.ch, max.klein@liverpool.ac.uk

Abstract

This text is an Addendum to the paper of the same title submitted on the LHeC, and the ERL development facility PERLE, to the European Particle Physics Strategy Update. Adding an electron-hadron scattering experiment to the LHC is expected to attract a collaboration strong enough to build and operate one extra LHC detector for concurrent eh and hh operation. The LHeC programme is of strong interest for the LHC community at large because of the striking synergy of eh with hh physics as described in the main paper. The present Addendum briefly describes the current ep/eA detector concept, and a timeline of its two-year installation is presented, which is commensurate with typical LHC shutdown durations. The ep interaction is free of pile-up and the event configuration cleaner than in pp, which tames the computing requirements for this detector with respect to the GPDs. Building and installing the ERL is estimated to take roughly a decade, which is consistent with the LHC future. The luminosity performance and operation profile are discussed, following recent official statements by CERN. Two ERL configurations are presented for electron beam energies ranging from 50 to 60 GeV, together with a physics evaluation of the importance to keep the electron energy high and a summary of the accelerator components in both cases. The cost is estimated to be around 1 billion CHF, subject to a final physics-energy-effort-cost optimisation at a suitable future time when the cost of the series production of the 802 MHz cavity-cryo modules can be more reliably determined. An Appendix sketches the design of the interaction region serving three beams. The LHeC physics, detector and machine developments, post the 2012 CDR, will be outlined in more detail in a report to appear in early 2019.

1 Interested Community

The LHeC has an outstanding programme on deep-inelastic electron-proton and electron-ion scattering (DIS) at the energy frontier, which surely will reassemble a community more than a decade after HERA was switched off. Building a new generation 4π acceptance detector in the twenties would be a major opportunity for a large number of institutions experimenting already or wishing to work at CERN, as the design and production, especially of the ATLAS and CMS detector upgrades for LS3 (2024+) is finishing. The LHeC detector is estimated to attract about a 1000 physicists, a bit more than worked on H1 and ZEUS. A high interest in the LHeC may be deduced from the representatives of 69 institutes who worked on the CDR [1] or from the authors of LHeC papers and new participants to workshops from a further about 50 institutes. As the linac-ring configuration would serve one interaction region, there have been thoughts expressed about building one common hardware base for two independent analysis collaborations.

The LHeC physics programme, with its PDF, electroweak, Higgs, BSM and Heavy-Ion parts, is highly synergetic with the HL-LHC physics. Building and operating a DIS experiment concurrent with the LHC is thus of prime interest for sustaining and extending the physics of the LHC facility. With this in mind one may view the LHeC experiment like a near detector for a long baseline neutrino facility. The LHC community at large would mostly profit from the concurrently operating LHeC and its physics outcome as sketched in the LHeC paper to which this Addendum belongs. The accelerator introduces a revolutionary technology with high power ERL and presents an outstanding opportunity for CERN and its partners to build and operate a new machine, 20 years after LHC began and probably two decades before a higher energy hadron-hadron machine may be built.

2 Timelines

2.1 Detector

2.1.1 Overview on Current Design

The asymmetry of the proton beam of energy E_p=7 TeV and the electron beam of E_e=60 GeV leads to very strong variations of the scattered electron and hadron final state energies, $E_e^{'}$ and E_h, in different regions of the detector, see Fig. 1. This has a considerable influence on the choice of detector technology and determines the geometric placements. Constraints arise from the circular-elliptical beam vacuum chamber housing the synchrotron radiation fan passing through the interaction region, see the Appendix. The design concept for the LHeC detector is a classic 4π acceptance collider detector using a solenoid magnetic field of 3.5 T. Its outer dimensions of 14 m length and 9 m diameter, one may compare with CMS ($21 \times 15\,\mathrm{m}^2$). The inclusive scattering kinematics can be reconstructed well in the complete (x, Q^2) plane, owing to the redundant determination of x and Q^2 from the angles (θ_e, θ_h) and energies ($E_e^{'}$, E_h) of the scattered electron and the hadronic final state, respectively. The reference LHeC detector has a single solenoid and an extended muon detector. Novel technology designs for combined tracking and calorimetry may allow muon detection without dedicated large scale chambers. There are different versions for the barrel calorimeters based on either crystal or Liquid Argon calorimeter technology. An alternative technology, in proton beam direction, uses Silicon as active material together with Pb or W absorbers. The pixel tracker extends up to ≈ 0.5 m radius to facilitate a dipole radius that is not too large and to limit the area of silicon required.

The design, sketched in Fig. 2 is developing based on the extensive study of the LHeC detector in the CDR [1] including forward and backward taggers. High precision Higgs physics and BSM searches have caused new, specific constraints on the calorimeter granularity and vertex tracker resolution. Salient features of the experiment, compared to pp, are the negligible pile-up, of 0.1, the clear distinction between neutral and charged current processes, and, notably, a radiation level which is about a factor of 100 lower than that for the hadron-hadron collisions. These features make the LHeC detector highly attractive for HV CMOS technology which so far is resistant only at the 10^{15} neutron equivalent level.

The current design serves as a baseline and for feasibility studies, it surely will be altered at a time of submitting a proposal, possibly following the strategy update.

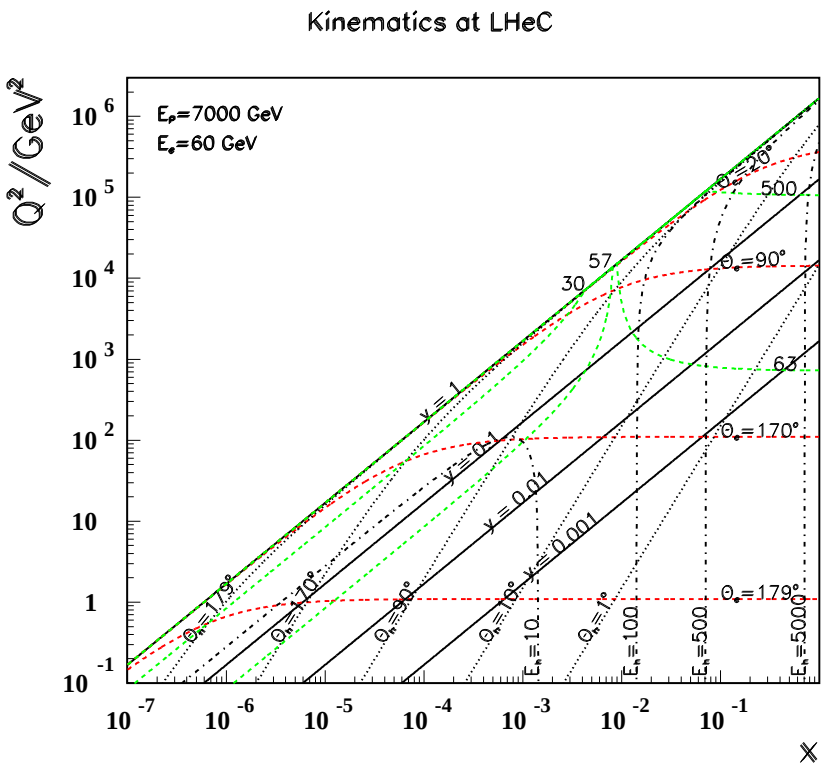

Figure 1: Lines of constant scattering angles and scattered energies for the electron (neutrino) and the hadronic final state in NC (CC) inclusive scattering at the default beam energies. Low E_p and low E_e special runs extend the kinematic coverage of the main detector at large x and towards lower Q^2, resp.

2.1.2 Detector assembly sequence and timeline

The usual constraints to HEP detector integration and assembly apply here even tighter since the detector has to be installed in a time duration essentially given by the machine shutdown for minimising the effect on the pp program. The strategy considered to minimise the installation period is to complete as much as possible the assembling and testing of the detector on surface, where the detector construction can proceed without impacting on the LHC physics runs. To save time, most of the detector components have been designed to match the handling means available on site, e.g. bridge crane in surface hall and experiment cavern. Nevertheless, a heavy lifting facility (about 300 ton capacity) will be rented for the time needed to lower the HCal barrel and plug modules. The IP for the LHeC is assumed to be P2, for an overview see Fig. 3.

The detector has been split in the following main parts for assembly purposes: i) Coil cryostat, including the superconducting coil, the two integrated dipoles and eventually the EMCal; ii) Five HCal tile calorimeter barrel modules, fully instrumented and cabled (5); iii) Two HCal plugs modules, forward and backward (2); iv) Two EMCal plugs, forward and backward (2); v) Tracker and Vertex detector (1); vi) Beam-pipe (1); vii) Central Muon detector (1 or 2) and viii) Endcaps Muon detector (2).

The full detector, including the Muon chambers, fits inside the former L3 Magnet Yoke, once the four large doors are taken away. The goal is to prevent losing time in dismantling the L3 Magnet barrel yoke and to make use of its sturdy structure to hold the detector central part on a platform supported by the magnet crown, whilst the Muon chambers will be inserted into lightweight structures (space-frames) attached to the inner surface of the octagonal L3 magnet. The installed detector, including machine elements, is illustrated in Fig. 3.

The sequence of installation has been studied in detail. The assembly on surface of the main detector

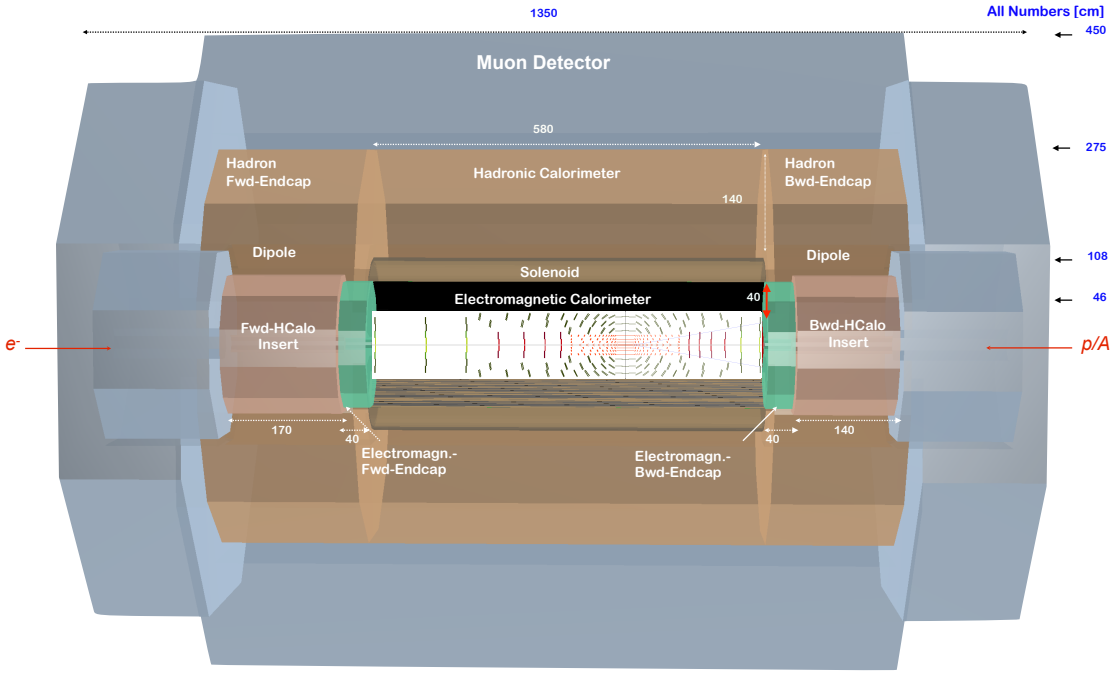

Figure 2: Current status of the LHeC central detector design. The detector is complemented by photon and electron taggers in the electron beam direction and by proton and neutron tagging forward spectrometers as were presented in the CDR [1].

elements, as previously defined, can start at any time, providing that the surface facilities are available, without sensible impact on the LHC run. The Coil system commissioning on site (T=0) could require 3 months and preparation for lowering 3 months, including some contingency. In the same time window, the L3 Magnet will be freed up and prepared for the new detector[1]. Detector component lowering is supposed to take one week per piece (15 pieces in total). Underground integration of the central detector elements inside the L3 Magnet would require about 6 months, cabling and connection to services some 8 to 10 months, in parallel with the installation of the Muon chambers, the Tracker and the Calorimeter Plugs. The total estimated time, illustrated in Fig. 4, from the starting of the testing of the Coil system on surface to the commissioning of the detector underground is thus 20 months. The beam-pipe bake out and vacuum pumping could take another 3 months and the final detector check-out one additional month. Some contingency (2 - 3 months in total) is foreseen at the beginning and the end of the installation period.

2.2 ERL Construction and Installation

An accelerator of the size of the ERL takes about a decade to be built as one knows from HERA (proposed in 1984, data taking in 1992) or XFEL (2008 beginning of construction, beam in 2017). Fig. 5 shows a draft timeline, from the CDR, for the production and installation of the LHeC. Depending on the final configuration chosen and with adjustment to the target dates and LHC shutdown sequence this scheme will be updated and become much more detailed. Mainly, the ERL can be installed independently of the LHC operation which is one of the major advantages as opposed to the ring-ring eh collider version previously also considered [1].

Following the CDR a further detailed study, consulting with external companies, has been made on the **Civil Engineering**. The Interaction Region (IR) for LHeC is assumed to be at LHC Point 2. As far as possible, any surface facilities have been situated on existing CERN land.

[1]The actual time depends on the level of activation and the procedure adopted for dismantling the existing detector.

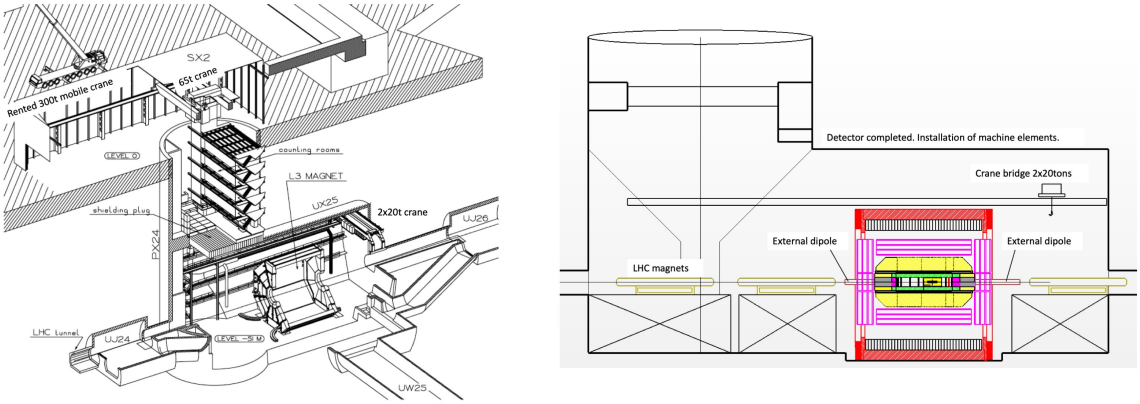

Figure 3: Left: LHC - P2 surface and underground facilities overview; Right: Fully installed LHeC detector.

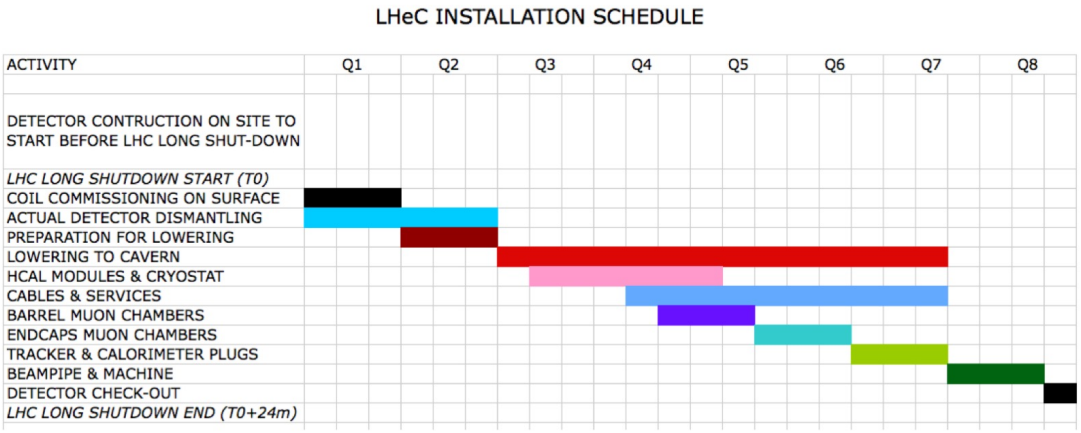

Figure 4: LHeC detector installation sequence in 8 quartals Qi.

The physical positioning for the project has been developed based on the assumption that the maximum underground volume possible should be housed within the Molasse Rock and should avoid as much as possible any known geological faults or environmentally sensitive areas. The shafts leading to any on-surface facilities have been positioned in the least populated areas.

The LHeC project is within the Geneva Basin, a sub-basin of the large North Alpine Foreland (or Molasse) Basin. The basin is underlain by crystalline basement rocks and formations of Triassic, Jurassic and Cretaceous ages. The Molasse, comprising an alternating sequence of marls and sandstones (and formations of intermediate compositions) is overlain by Quaternary glacial moraines related to the Wurmien and Rissien glaciations.

The Energy Recovery Linac will be located around the St.Genis area of France, injecting directly into the LHC ALICE Cavern at Point 2. Approximately 10 km of new tunnels (5 m and 6 m diameter), 2 shafts and 7 caverns will be required. The majority of civil engineering work can be pursued while LHC is operational.

In addition to the minimum required length for the two linacs and the return arcs, we assume a required space of 400 m in each straight for the beam delivery system [spreader and combiner sections] and the beam dumps and a total length of 400 m for the transfer lines for the connection of the ERL to the hadron collider facility. Furthermore, we require a total length of 2140 m for a parallel RF gallery and a total of 50 waveguide

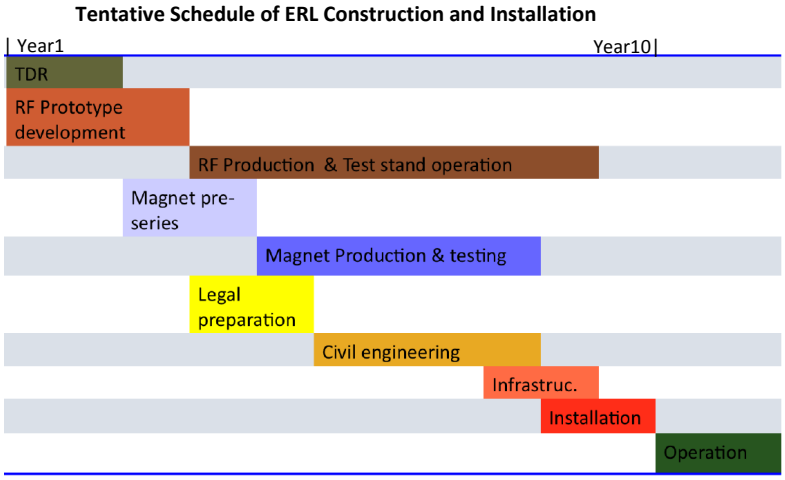

Figure 5: Sketch of the production and installation sequence for the ERL.

Parameter [unit]	LHeC CDR	ep at HL-LHeC	ep at HE-LHC	ep at FCC-hh
E_p [TeV]	7	7	13.5	50
E_e [GeV]	60	60	60	60
$\sqrt{s}$ [TeV]	1.3	1.3	1.7	3.5
bunch spacing [ns]	25	25	25	25
protons per bunch [10^9]	1.7	2.2	2.5	1
$\gamma\epsilon_p$ [μm]	3.7	2	2.5	2.2
electrons per bunch [10^9]	1	2.3	3	3
IP beta function β_p^* [cm]	10	7	10	15
Hourglass factor H_{geom}	0.9	0.9	0.9	0.9
pinch factor H_{b-b}	1.3	1.3	1.3	1.3
proton filling H_{coll}	0.8	0.8	0.8	0.8
peak luminosity [$10^{33} cm^{-2} s^{-1}$]	1	8	12	15

Table 1: Parameters of the various ep configurations: LHeC CDR; ep at HL-LHC; ep at HE-LHC and ep at FCC-hh, from [2]. The luminosity for electron-ion scattering is estimated to be $8 \cdot 10^{32}\,\mathrm{cm}^{-2}\mathrm{s}^{-1}$, leading to an integrated luminosity in e-Pb scattering of about $10\,\mathrm{fb}^{-1}$, ten times larger than HERA's ep luminosity in a small fraction of its running time.

connections between the two straight tunnel structures. The Linac sections and the RF tunnel are assumed to be separated by 10 m of rock, therefore, each waveguide will require a borehole with a length of 10m and diameter of 1 m.

2.3 Operation and Luminosity Profile

The luminosity prospects for electron-proton and electron-ion scattering at the LHeC and its possible successors have been studied in detail recently and are summarised in [2] from which Tab. 1 is taken.

This has been used as input to an initial evaluation of the integrated luminosity and operation profile, published by CERN [3]. A crucial ingredient is the appropriate design of the interaction region. It is crucial for the luminosity performance, Tab. 2, that β^* values of and below 10 cm are achievable, which is within reach, see Appendix. For the LHeC three running periods have been assumed as is detailed in Tab. 2:

- LHeC during LHC Run 5: initial operation concurrent to pp, yielding $50\,\mathrm{fb}^{-1}$. The integrated luminosity already from this initial run is 100 times larger than HERA's, with collisions at much higher

energies. This therefore provides the bulk of the novel DIS programme, delivering essentially all of the precision QCD and electroweak input required to complement the GPD pp programme, prior to LS5;

- LHeC during LHC Run 6: design operation concurrent to pp, adding another 175 fb^{-1}. This provides Higgs physics at the 2 % precision level, roughly, and extends to BSM sensitive processes;
- A final LHeC run in dedicated operation without pp adds a further 650 fb^{-1}. This is the era of high-precision Higgs physics and rare processes.

If the LHeC begins operation after LS4, it had, according to current plans, seven years of concurrent ep and pp operation with the HL-LHC if the LHC Run 6 lasts for four years. The total integrated luminosity over all three running modes comes close to 1 ab^{-1}. Other short runs at low electron and proton energies, as well as running periods of the LHeC with ions are also possible.

For the HE-LHC and the FCC, one can envisage concurrent operation from the start of the pp run, lasting for about two decades. This provides about 2 ab^{-1} as a realistic estimate for the integrated luminosity.

Parameter	**Unit**	**Initial: Run 5**	**Design: Run 6**	**Dedicated**
Brightness $N_p/(\gamma\epsilon_p)$	10^{17} m^{-1}	2.2/2.5	2.2/2.5	2.2/2.5
electron beam current I_e	mA	15	25	50
proton β^*	m	0.1	0.07	0.07
peak luminosity	10^{34} $\text{cm}^{-2}\text{s}^{-1}$	0.5	1.2	2.4
p beam lifetime	h	16.7	16.7	100
fill duration	h	11.7	11.7	21
turnaround time	h	4	4	3
overall efficiency	%	54	54	60
Physics time / year	days	160	180	185
Annual integrated lumin.	fb^{-1}	20	50	180

Table 2: Parameters and expected performance for the LHeC data taking periods, from [3].

3 Energy Range, Configurations and Cost

The CDR [1] has chosen 60 GeV as the default electron beam energy, E_e leading to a 9 km circumference configuration which is sketched in the main LHeC paper. For adjustment with the LHC timing the ERL circumference has to be a $1/n$ fraction of the LHC circumference of 27 km. For this submission we have considered an energy range between 50 (n=5, or n=4, the SPS size, to allow for upgrading E_e) and 60 GeV (n=3). Lowering the energy from 60 to 50 GeV would reduce the total cost by about one third to approximately one billion CHF. The cost is dominated by the SRF structure and an exact estimate has to be deferred until one has a reliable estimate on the cost of an 802 MHz cryo module when produced in series[2]. It also depends on the gradient and the Q_0 achieved in fully equipped modules. The wall-plug power of the ERL was limited to 100 MW. The annual operation cost of the ERL is estimated to be 14.5 million CHF for an operation of 200 days. The final choice of the energy will emerge when one re-discusses the physics, effort and cost interrelations in the light of later actual developments. Physics findings at the LHC or firm new theoretical predictions may require an energy higher than 60 GeV. In any case, one may conclude that the cost of the electron upgrade of the LHC will be (and should be) small compared to the total investment in the LHC. Since the LHeC utilises the existing hadron beam, it turns out to be indeed cost effective, as compared to any of the proposed future hadron-hadron and e^+e^- high energy colliders. The following two sections present a brief discussion of physics considerations followed by a comparative study of the 60 and 50 GeV energy configurations.

[2]A first cost estimate using available information such as from XFEL and LCLS-II has been summarised in [4].

3.1 Physics Potential and the Choice of the Electron Beam Energy

The cost estimate as discussed above makes clear that for energies above about 60 GeV, a non-linear cost rise sets in. One finds that already with $E_e = 80$ GeV the cost reaches O(3) BSF. It therefore is considered that the electron beam energy may not be significantly higher than 60 GeV. This has also a practical side, because of the considerable load of synchrotron radiation in the IR which requires head-on collisions, i.e. to bend the beam in and out.

Three main physics topics have been considered in the choice of the electron beam energy.

- First, the precision measurements on the Higgs couplings. The strong impact of the LHeC on testing the SM Higgs properties relies on the precision determination of the dominant $H \to b\bar{b}$ channel. With $1\,\mathrm{ab}^{-1}$ luminosity and $E_e = 60$ GeV one estimates the uncertainty of the signal strength (μ_b) measurement in charged currents to be 0.8 %. Reducing E_e worsens the acceptance somewhat and reduces the cross section linearly. At 50 GeV the μ_b uncertainty becomes 1.1 % and it increases to 1.8 % at 30 GeV. It is to be noted that factors of two matter when one compares the pp & ep Higgs potential to electron-positron colliders. The value of LHeC as a competitive Higgs facility is directly proportional to E_e and 60 GeV an optimum choice.

- Second, the potential for BSM physics. This is naturally directly proportional to the available energy. For illustration, we have considered the measurement of the ttH coupling which is about 17 % accurate at 60 GeV and worsens to 31 % at 40 GeV. The discovery potential for an anomalous tqH coupling reduces from 0.5 % over 3.2 % to 22 % for 60, 50 and 40 GeV electron beam energy, respectively. There may occur new high energy phenomena, as was the case with the sudden appearance of a 750 GeV 'ghost' state. An LHeC which chose a too economic version could miss out such effect, which calls for leaving room for upgrading by choosing the tunnel dimensions not too small. These considerations, albeit not complete, also suggest to keep the energy as high as is affordable, and not lower than 50 GeV

- Third, the potential for low x physics. The discovery and confirmation or the reject of the gluon saturation hypothesis requires a one percent precise measurement of the longitudinal structure function [5]. The sensitivity on F_L is proportional to the inelasticity ys squared, i.e. it requires to measure the DIS cross section up to $y \simeq 1 - E'/E_e = 0.9$. Since the electron identification becomes difficult for a few GeV of scattered electron energy E', one requires, refering to experience on H1, E_e to be larger than about twice the HERA beam energy.

A tentative summary of these considerations has been that 60 GeV is indeed an optimum value. If necessary it may be reduced to 50 GeV to economise funding also reducing the CE and overall effort, see below Sect. 3.2. With 50 GeV one would want to choose a circumference of the LHeC ERL of 1/4. This made LHeC as large as the SPS and left room for an energy upgrade to perhaps 55 GeV should that become important.

3.2 Lattice and Components for 60 and 50 GeV Electron Beam Energy

The 60 GeV baseline ERL features a racetrack composed of two 1 km long linacs. In each linac alternating quadrupoles are placed every two cryomodules providing periodic FODO configuration for the lowest energy pass. Energy recovery in a racetrack topology explicitly requires that both the accelerating and decelerating beams share the individual return arcs. This in turn imposes specific, mirror-symmetric requirements for TWISS function at the linacs ends. All six 180° arcs fit a tunnel of 1 km radius, with the dipole filling factor of 76% (effective bending radius of 760 m). Their lattice cells adopt a flexible momentum compaction optics. The tuning of each arc takes into account the impact of synchrotron radiation at different energies. At the highest energy, it is crucial to minimize the emittance dilution; therefore, the cells are tuned to minimize the dispersion in the bending sections, as in a theoretical minimum emittance lattice. At the lowest energy, one compensates for the bunch elongation with a negative momentum compaction setup which, additionally, contains the beam size. The intermediate energy arcs are tuned to a double bend achromat lattice, offering a compromise between isochronicity and emittance dilution. Before and after each arc, matching sections adjust the optics from and to the linacs. Adjacent to these, additional cells are placed, hosting the RF compensating sections. The compensation makes use of a second harmonic field to replenish the energy

lost by synchrotron radiation for both the accelerating and the decelerating beam, therefore guaranteeing the same beam energy at a given arc entrance. The spreaders, following each linac, separate bunches at different energies and route them to the corresponding arcs (mirror-symmetric recombiners do just the opposite). The spreader/recombiner design consists of a vertical bending magnet, common for all beams, that initiates the separation. The highest energy beam is brought back to the horizontal plane with a chicane. The lower energies are captured with a two-step vertical bending adopted from the CEBAF design. Accelerator components for the baseline ERL are collected in Tab. 6. One may consider a downsized ERL

60 GeV LHeC Recirculator

Section	Horizontal Dipoles			Vertical Dipoles			Quadrupoles			RF Cavities		
	Number	*Field*	*Mag. Length*	*Number*	*Field*	*Mag. Length*	*Number*	*Gradient*	*Mag. Length*	*Number*	*Frequency/Cell*	*RF Gradient*
LINAC 1							35	2.3	1.0	544	802/5	20.0
LINAC 2							35	2.3	1.0	544	802/5	20.0
Arc 1	584	0.047	4.0	8	0.61	4.0	254	11.1	1.0			
Arc 2	534	0.092	4.0	6	0.89	4.0	234	21.2	1.0			
Arc 3	584	0.147	4.0	6	1.10	4.0	254	29.1	1.0	6	1604/9	30.0
Arc 4	534	0.217	4.0	6	1.47	4.0	234	32.6	1.0	6	1604/9	30.0
Arc 5	584	0.227	4.0	4	0.92	4.0	252	40.7	1.0	18	1604/9	30.0
Arc 6	584	0.271	4.0	4	1.79	4.0	252	48.9	1.0	36	1604/9	30.0
Total	**3404**			**34**			**1550**			**1154**		

Units: meter (m), Tesla (T), T/m, MHz, MV/m

Figure 6: Components of the 60 GeV ERL at 1/3 of the LHC circumference, with 136 cryomodules per linac.

at 50 GeV, which has the same performance in terms of synchrotron radiation effects (578 m radius arcs, corresponding to 1/5 of the LHC circumference); its components are summarised in Tab. 7.

50 GeV LHeC Recirculator

Section	Horizontal Dipoles			Vertical Dipoles			Quadrupoles			RF Cavities		
	Number	*Field*	*Mag. Length*	*Number*	*Field*	*Mag. Length*	*Number*	*Gradient*	*Mag. Length*	*Number*	*Frequency/Cell*	*RF Gradient*
LINAC 1							29	1.9	1.0	448	802/5	20.0
LINAC 2							29	1.9	1.0	448	802/5	20.0
Arc 1	344	0.039	4.0	8	0.51	4.0	158	9.3	1.0			
Arc 2	294	0.077	4.0	6	0.74	4.0	138	17.7	1.0			
Arc 3	344	0.123	4.0	6	0.92	4.0	158	24.3	1.0	6	1604/9	30.0
Arc 4	294	0.181	4.0	6	1.23	4.0	138	27.2	1.0	6	1604/9	30.0
Arc 5	344	0.189	4.0	4	0.77	4.0	156	33.9	1.0	18	1604/9	30.0
Arc 6	344	0.226	4.0	4	1.49	4.0	156	40.8	1.0	30	1604/9	30.0
Total	**1964**			**34**			**962**			**956**		

Units: meter (m), Tesla (T), T/m, MHz, MV/m

Figure 7: Components of the 50 GeV ERL at 1/5 of the LHC circumference with 112 cryomodules per linac.

4 Authors

The results on which the LHeC paper submission rests have been obtained in many years of work by a large, interested community of several hundred physicists, experimentalists, theorists and accelerator scientists, from about 120 different institutes. This submission is made gratefully on their behalf. The text was prepared by the Coordination Group and the Physics Convenors with several parts contributed by esteemed colleagues outside this coordination. The LHeC paper was circulated to 650 colleagues the comments of which where hopefully correctly considered. There will be an update of the CDR published early 2019, with enough time and print space for an appropriate author list. The LHeC and PERLE papers were discussed with and endorsed by the International Advisory Committee chaired by Herwig Schopper. They were also

seen by the Chair of the FCC International Advisory Committee, Guenter Dissertori (ETH Zuerich), and the FCC Coordination, to which several of the LHeC Coordination Group members belong. The PERLE paper had been in time sent to the representatives, usually the Accelerator Directors, of the Collaborating Institutes. The organisation of the LHeC development is visible from Fig. 8.

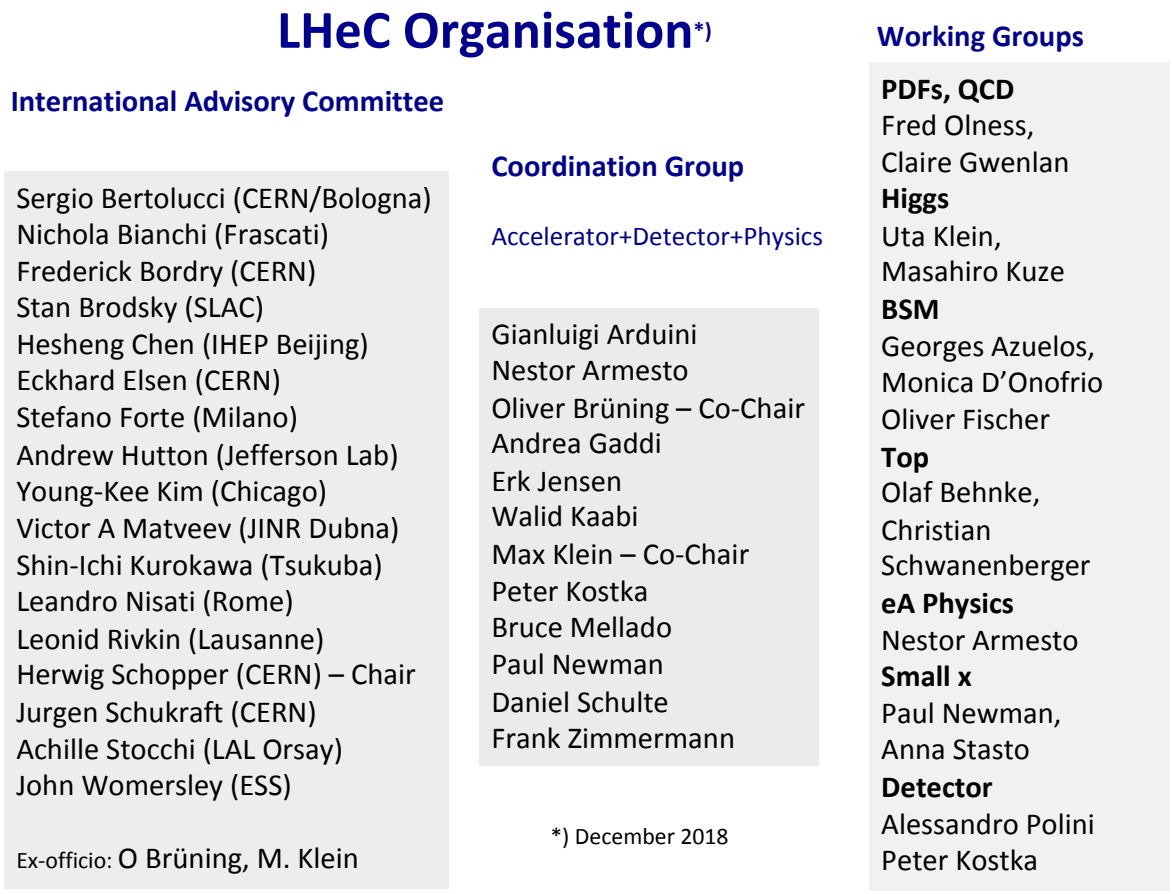

Figure 8: Steering Committees of the LHeC, see text.

Appendix: Interaction Region

The current design of the interaction region is shown in Fig. 9. Strong quadrupole septa focus the colliding proton beam at the interaction point. Since the electron beam has a significantly lower beam rigidity it must pass these magnets in the field free region. This leads to an angle of 10.6 mrad between the two incoming colliding beams. Dipoles around the IP bend the electron beam into head-on collisions with the proton beam and separate the two beams after the IP. The required field of these dipoles is determined by the L^* and the minimum separation of the electron and the colliding proton beam at the first quadrupole Q1. With an L^* of 15 m and an optimized dipole length of 10 m [6], a field of 0.21 T is sufficient to provide 106 mm separation, enough to pass Q1 in the field free region. Although the dipoles are rather weak, the electron beam energy of 60 GeV and beam current of 20 mA lead to a synchrotron radiation power of 83 kW at a critical energy of 513 keV in the immediate vicinity of the detector. If the beam energy is reduced to 50 GeV the power decreases to 40 kW and the critical energy to 296 keV.

With updated quadrupole septum designs featuring Nb_3Sn technology and self-contained coils for Q1 as well as actively shielded quadrupoles for the subsequent magnets (see Table 4), the interaction region design achieves a minimum β^* of 10 cm. The integration of the LHeC interaction region into the HL-LHC ring shows promising results: Chromaticity correction is possible for $\beta^* = 7$ cm using an achromatic telescopic squeezing scheme extending over one additional arc. However, a $\beta^* \simeq 7$ cm will require apertures 15 %

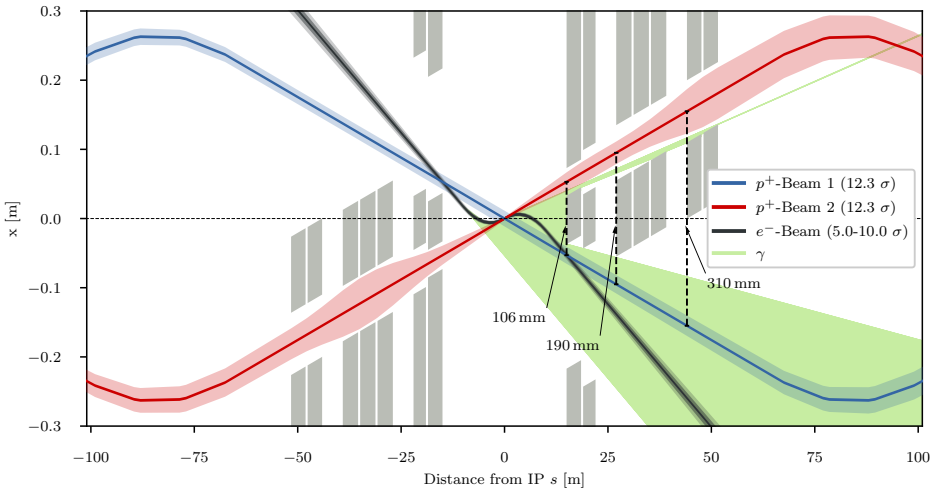

Figure 9: Layout of the LHeC interaction region with $\beta^* = 10\,\text{cm}$.

Magnet	Gradient [T/m]	Free aperture radius [mm]
Q1a	252	20
Q1b	164	32
Q2	186	40
Q3	175	45

Table 3: Parameters of the quadrupole septa [7].

larger than listed in Table 4 at comparable gradients. Dynamic aperture for the case with $\beta^* = 10\,\text{cm}$ is just above the HL-LHC target with $10.1\,\sigma$ with the aid of non-linear correctors, while the more challenging case, tentatively studied, for $\beta^* = 7\,\text{cm}$ resulted in $9.6\,\sigma$.

References

[1] J. L. Abelleira Fernandez et al. A Large Hadron Electron Collider at CERN: Report on the Physics and Design Concepts for Machine and Detector. *J. Phys.*, G39:075001, 2012.

[2] Oliver Bruening et al. FCC-eh Baseline Parameters. *FCC-ACC-RPT-0012*, 2017.

[3] Frederick Bordry et al. Machine Parameters and Projected Luminosity Performance of Proposed Future Colliders at CERN. arXiv:1810.13022, 2018.

[4] O. Bruening. A Report on the ERL Cost. *CERN-ACC-2018-XXX, to appear*, 2018.

[5] Max Klein. Future Deep Inelastic Scattering with the LHeC, arXiv:1802.04317. 2018.

[6] Roman Martin and Rogelio Tomas Garcia. Length optimization of the detector region dipoles in LHeC and FCC-eh. Technical Report CERN-ACC-2018-0042, CERN, Geneva, Oct 2018.

[7] Brett Parker. Latest Developments and Progress on the IR Magnet Design. Presented at the Electrons for the LHC - LHeC/FCCeh and Perle Workshop, June 2018.